Published in final edited form as:
Am J Physiol Renal Physiol. 2007 March ; 292(3): F1065–F1072. doi:10.1152/ajprenal.00229.2006.

Origin of spontaneous activity in neonatal and adult rat bladders and its enhancement by stretch and muscarinic agonists

A. Kanai[1,2], **J. Roppolo**[2], **Y. Ikeda**[1], **I. Zabbarova**[1], **C. Tai**[2], **L. Birder**[1,2], **D. Griffiths**[1], **W. de Groat**[2], and **C. Fry**[3]

[1]Department of Medicine, University of Pittsburgh School of Medicine, Pittsburgh, Pennsylvania

[2]Department of Pharmacology, University of Pittsburgh School of Medicine, Pittsburgh, Pennsylvania

[3]Institute of Nephrology and Urology, University College London, London, United Kingdom

Abstract

This study examined the origin of spontaneous activity in neonatal and adult rat bladders and the effect of stretch and muscarinic agonists and antagonists on spontaneous activity. Rats were anesthetized and their bladders were excised, cannulated, and loaded with voltage- and Ca^{2+}-sensitive dyes. Intracellular Ca^{2+} and membrane potential transients were mapped using photodiode arrays in whole bladders, bladder sheets, or cross-section preparations at 37°C. Intravesical pressure was recorded from whole bladders. In neonatal bladders and sheets, spontaneous Ca^{2+} and electrical signals arose at a site near the dome and spread in a coordinated manner throughout the bladder with different dome-to-neck conduction velocities (Ca^{2+}: 3.7 ± 0.4 mm/s; membrane potential: 46.2 ± 3.1 mm/s). In whole bladders, optical signals were associated with spontaneous contractions (10–20 cmH_2O). By contrast, in adult bladders spontaneous Ca^{2+} and electrical activity was uncoordinated, originating at multiple sites and was associated with smaller (2–5 cmH_2O) contractions. Spontaneous contractions and optical signals were insensitive to tetrodotoxin (2 μM) but were blocked by nifedipine (10 μM). Stretch or low carbachol concentrations (50 nM) applied to neonatal whole bladders enhanced the amplitude (to 20–35 cmH_2O) of spontaneous activity, which was blocked by atropine. Bladder cross sections revealed that Ca^{2+} and membrane potential transients produced by stretch or carbachol began near the urothelial-suburothelial interface and then spread to the detrusor. In conclusion, spontaneous activity in neonatal bladders, unlike activity in adult bladders, is highly organized, originating in the urothelium-suburothelium near the dome. Activity is enhanced by stretch or carbachol and this enhancement is blocked by atropine. It is hypothesized that acetylcholine is released from the urothelium during bladder filling to enhance spontaneous activity.

Keywords

optical mapping; pacemaker activity; urothelium; voltage- and Ca^{2+}-sensitive dyes

Bladder and Urethral Smooth muscle displays spontaneous contractile activity during the filling phase, which is tonic in the urethra but phasic in the detrusor. While urethral activity may contribute to closing pressure, the role of detrusor activity is unclear. In normal adult bladders, their high compliance may dampen the pressure changes associated with this

Address for reprint requests and other correspondence: A. J. Kanai, Dept. of Medicine, Univ. of Pittsburgh School of Medicine, A1224 Scaife Hall, Pittsburgh, PA 15261 (ajk5@pitt.edu)..

activity, which could locally shorten muscle bundles to maintain optimal bladder shape as it fills (4).

Whole rat bladders and isolated strips from postnatal animals (1–3 wk) exhibit high-amplitude spontaneous contractions, which may promote voiding as neural control is still immature (17,18). While every spontaneous contraction does not result in voiding, large-amplitude spontaneous contractions may enhance the likelihood of urine loss. Thereafter, supraspinal neural mechanisms develop to control bladder reflexes and voluntary voiding as intrinsic bladder activity declines (23,27). Spontaneous activity is myogenic, as it occurs also in isolated detrusor smooth muscle cells (9). It may originate from the smooth muscle cells themselves or accessory cells such as interstitial cells that have been demonstrated surrounding the muscle bundles and in the suburothelial space (19,26).

Antimuscarinic drugs are the preferred pharmacological treatment for urgency, frequency, and urge incontinence associated with detrusor overactivity (1,5,16,20,22,29). Their mechanism of action, however, is unclear as they act during the filling phase when parasympathetic activity is low (2,3), and they are more effective in suppressing bladder activity in patients with overactive bladder symptoms than in normal subjects (31). One hypothesis is that acetylcholine (ACh), along with ATP, is released from a nonneuronal source, stimulated by stretch of the bladder wall during filling. In pathological bladders, this may lead to overactive bladder symptoms and stimulate responses to cause contractions. One potential source of ACh is the urothelial cells (30), which also exhibit a greater density of muscarinic receptors than detrusor myocytes (6). We addressed some of these questions by developing a system to record and map simultaneous changes of intracellular Ca^{2+} and membrane potential at multiple sites in the bladder wall. Activation of urothelial muscarinic receptors could lead to the release of a number of urothelial transmitters, including ATP, that could ultimately excite afferent nerves or myofibro-blasts in the suburothelium or detrusor. Accordingly, important questions are the source and site-of-action of nonneuronal ACh and the features unique to the overactive bladder that make it amenable to antimuscarinic therapy.

MATERIALS AND METHODS

Experimental preparations

Bladders from neonatal (3–21 days old) and mature (4 mo old) rats were used. Neonates were euthanized by decapitation and their bladders were harvested. Adults were anesthetized with 2.5% halothane, their bladders were excised, and then euthanized using inhalational CO_2. Bladders were cannulated (22-gauge needle) and loaded intravesically with voltage (10 μM Di-4-ANNEPS, 15 min, 25°C)- and Ca^{2+} (5 μM Rhod-2-AM, 15 min, 37°C)-sensitive dyes.

Whole bladders were mounted in a Peltier-regulated chamber, cast, and machined from thermally conductive epoxy (Fig. 1*B*). The cannula was connected to a transducer at the level of the bladder to record intravesical pressure. After zeroing to atmosphere, the bladder was filled with Tyrode's solution to a pressure of 2 cmH_2O. Electrically stimulated responses were evoked via platinum electrodes using 20-s trains (50 Hz, 0.25 ms, 140-V pulses). For whole bladder sheet preparations, bladders were cut open longitudinally along the dorsal aspect and mounted with the luminal surface upwards on a two-piece rack (see Fig. 7A). The rack had pins inscribing an 8-mm-diameter circle, where one-half was fixed, and the other slid on polished stainless steel rods. The movable portion was connected to a tension transducer mounted on a micromanipulator. Bladders were brought to resting length (L_0) by stretching along the outlet-to-dome axis by moving the manipulator and then stretched by 10%. This permitted normalization of data between different preparations.

Stretch of the sheet to evoke Ca^{2+} and membrane potential transients was achieved by a similar method. Bladder cross sections were pinned vertically in a chamber that allowed us to image across the wall (see Fig. 8*A*). Preparations were superfused at 0.5 ml/min, with a modified Tyrode's solution containing (in mM): 113 NaCl, 4.7 KCl, 2.5 $CaCl_2$, 1.2 $MgSO_4$, 25 $NaHCO_3$, 1.2 KH_2PO_4, 11.5 glucose, at pH 7.4, bubbled with 95% O_2-5% CO_2. The superfusate temperature was maintained at 37 ± 0.5°C. Carbachol and tetrodotoxin were added from 1 mM aqueous stocks either directly onto the preparation or to the superfusate. 2,3-Butanedione monoxamine (BDM) was added from a stock to Tyrode's solution to achieve a final concentration of 5 mM. All reagents were from Sigma, except the fluorescent dyes, which were supplied by Molecular Probes.

Optical apparatus

Light from a 100-W tungsten halogen lamp was collimated, passed through a 540 ± 40-nm excitation filter, and focused onto the surface of the preparation (Fig. 1*A*). Tissue fluorescence was collected with a camera lens (Nikon *f* 1:1.2/50 mm for intact bladders and sheets or Fujinon *f* 1:0.85/25 mm for cross sections) and passed through a 45° long-wave pass dichroic filter, with a cut-off at 635 nm. Fluorescence from the Ca^{2+} probe was below 635 nm and was reflected onto a 16 × 16 photodiode "Ca^{2+} array." The signal from the voltage probe was above 635 nm and transmitted to a similar "voltage array." Each photodiode had a sensing area of 0.95 × 0.95 mm, with an inter pixel spacing of 1.1 mm. The image of the bladder was focused onto the arrays, with each photodiode detecting light from ~625 × 625 μm (intact bladders and sheets) or ~62.5 × 62.5 μm (cross sections) areas. It was thus possible to map action potential and Ca^{2+} transients (generally for 60 s) over the mucosal or serosal surface or across the bladder wall from mucosa to serosa. The outputs from the photodiode arrays were amplified (1–1,000 times) and digitized (14 bits); the maximum sampling rate was 4,000 frames/s and the signal:noise ratio was ~200:1.

Signal analysis

The conduction delays of the Ca^{2+} and membrane potential (V_m) transients were determined from the cross-correlation analysis of their waveforms. This was accomplished by selecting one channel with an early response and using cross-correlation analysis to determine the delays. A time window was used to limit our analysis to a single bladder contraction. To visually represent Ca^{2+} or V_m transients as propagating waves, we generated isochrones linking points on the bladder with similar conduction delays, as shown in Fig. 1*D*.

Statistical analysis

Student's *t*-test was used to validate spatial and temporal differences between Ca^{2+} or V_m transients (e.g., between the dome and the neck). The data are represented as means ± SD.

RESULTS

The optical imaging system mapped electrical activity and Ca^{2+} transients over the entire serosal surface, in intact bladders (see Figs. 1, 4, and 5), the mucosal face in sheets (see Fig. 7), or across the wall from mucosa to serosa (see Fig. 8). It was thus possible to determine where spontaneous activity was initiated, how it spread, and what factors might modulate it. Part A shows a schematic of the experimental system and part B shows a representation of the 16 × 16 photodiode array grid, superimposed over the image of neonatal rat bladder. Spontaneous Ca^{2+} data are shown in part C and converted to a gray scale isochronal map in part D, to visualize spread of activity (darker with increasing delay). To construct isochronal maps from the component traces, the transient showing the earliest onset was taken as the initiation site, and lines of equal delay (isochrones) were drawn using the remaining traces. In these maps, white is the first and black is the last region to undergo Ca^{2+} transients.

Figure 1*D* demonstrates that in this neonatal bladder, there was focal initiation near the dome followed by an organized spread of activity toward the neck (see also Fig. 4), similar results were seen in $n = 7$ neonatal bladders.

Spontaneous activity and the effects of tetrodotoxin and nifedipine

Figure 2 shows a pressure recording from an adult rat bladder, with low-amplitude spontaneous activity (2–5 cmH_2O) and a larger tetrodotoxin (TTX)-sensitive (2 μM) electrically evoked (EFS) response (70 cmH_2O). The electrically evoked response was blocked by 2 μM TTX, but spontaneous activity was unaffected. Nifedipine (10 μM) did however block spontaneous activity (not shown). Figure 3 shows recordings of spontaneous activity from a neonatal bladder. The spontaneous contractions were much greater (10–20 cmH_2O), but at a slower rate, compared with adult bladders. These spontaneous contractions were similarly TTX insensitive but nifedipine sensitive.

Spontaneous electrical and intracellular Ca^{2+} transients in neonatal and adult bladders

The bottom record in Fig. 4 shows a series of five large-amplitude, spontaneous pressure waves in a neonatal bladder. The top portion shows the earliest Ca^{2+} transients associated with the middle three pressure changes and the derived isochronal maps. Two important observations were made: *1*) the same area (white region) exhibited the earliest transient in all three events, indicating a stable focus; and *2*) the isochrones spread across almost the whole visible surface of the bladder. An average conduction velocity calculated in the dome-to-neck axis was 4 mm/s. Similar analysis of the Ca^{2+} transients from seven bladders yielded a mean value of 3.7 ± 0.4 mm/s. Shown also is a corresponding membrane potential isochronal map for the middle pressure change, with the display of the earliest event. The transient itself was shorter than the Ca^{2+} trace, but originated from a similar site spreading also across a substantial fraction of the visible surface. However, the conduction velocity in the same axis was faster (45 mm/s), with a mean value of 46.2 ± 3.1 mm/s ($n = 7$).

By contrast, in adult bladders (Fig. 5) the pressure changes were more rapid, smaller, and more variable in amplitude. This irregularity was reflected in the Ca^{2+} transients and their isochronal maps. The maps showed multiple, small focal origins that changed position constantly in successive pressure events. When calculation of a dome-neck conduction velocity was possible, the average value was 1.5 ± 0.7 mm/s ($n = 7$). Similar fragmentation of membrane potential maps was also observed, with an average velocity of 27.3 ± 6.2 mm/s, again significantly greater than for corresponding Ca^{2+} maps.

Control experiments, to address the possibility that the fluorescence signals were motion artifacts due to bladder contractions, used 5 mM BDM in Tyrode's solution. This agent suppresses contraction, in part, through prevention of actomyosin interactions (21). Figure 6 shows an example from a neonatal bladder in which the spontaneous pressure transients were reversibly abolished by BDM. Above the pressure traces are shown isochronal Ca^{2+} maps of the bladder surface, derived from the array of Ca^{2+} transients superimposed over the map. The traces were obtained before, during, and after BDM application. The data show that spontaneous Ca^{2+} waveforms persisted in the presence of BDM despite the abolition of pressure traces. Indeed, one of the strengths of the optical imaging approach is that we can record/demonstrate spontaneous activity in the absence of bladder pressure, which is not possible using a pressure transducer.

Isochronal maps in bladder sheets and bladder cross-sections: effects of mechanical stimulation and carbachol

Mechanical stretch of a neonatal bladder sheet from dome to neck (Fig. 7*A*) generated simultaneous Ca^{2+} (Fig. 7B) and membrane potential waves over the visible surface ($n = 4$).

The preparation was stretched by 10% of its length within 5 s during signal acquisition. Application of carbachol (50 nM) to the center of the preparation also generated concentric Ca^{2+} (Fig. 7C) and membrane potential waves, spreading out from the site of application (n = 5). Conduction velocities of the Ca^{2+} and membrane potential waves in the neck-dome axis were, respectively, 4.7 ± 0.7 and 47 ± 7.5 mm/s for stretch and 6.7 ± 2.1 and 52 ± 6.1 mm/s after carbachol application. The Ca^{2+} or membrane potential conduction velocities elicited by the two interventions were not significantly different from each other nor were they different from their respective velocities for spontaneous contractions. This implies that the spontaneous or interventional Ca^{2+} and membrane potential waves propagated by similar mechanisms. Before and several seconds after the application of stretch or carbachol, spontaneous Ca^{2+} (Fig. 7*D*) and membrane potential waves were observed which began in the dome and spread toward the neck of the bladder sheet. Similar experiments were conducted using adult bladders (Fig. 7, *E*–*G*) where the most notable differences were that spontaneous activity began simultaneously at multiple sites and exhibited slower conduction velocities, comparable to what was observed and recorded in Fig. 5 from intact adult bladder preparations.

The preceding experiments did not give any information as to where in the bladder wall the transients were initiated and/or enhanced. This information was obtained by analyzing activity in transverse sections of neonatal bladders (Fig. 8*A*). Mechanical stimulation at the point marked by the asterisk in Fig. 8*B* evoked Ca^{2+} and membrane potential waves that spread rapidly in the urothelial-suburothelial regions, then propagated in the transverse direction toward the detrusor layer, but after a delay of 1–2 s. A similar preference of propagation was observed if carbachol was added to the preparation (Fig. 8*C*). The drawing in Fig. 8*D* depicts the layers of the bladder wall shown in Fig. 8, *A*–*C* (and also Fig. 8, *E*–*F*). In the presence of atropine (2 μM), the effects of stretch and carbachol on the urothelium-suburothelium and detrusor were blocked and no isochronal maps could be constructed in either neonatal or adult preparations (n = 4). Alternatively, in the presence of the purinergic receptor antagonist, suramin (50 μM), the stretch/carbachol-induced activity seen in the urothelium-suburothelium was unaffected, but the spread of activity into the detrusor was blocked (n = 4). Similar experiments were conducted using transverse sections of adult bladders, where focal stimulation (Fig. 8*E*, at the asterisk) and the addition of 50 nM carbachol (Fig. 8*F*) also evoked Ca^{2+} and membrane potential waves that spread in the urothelial-suburothelial regions. However, these atropine (2 μM)-sensitive waves did not propagate into the detrusor (n = 4). In Fig. 8, *E* and *F*, spontaneous activity can be seen initiating in the detrusor, in this example from sites near the serosal surface of the bladder wall.

The findings regarding stretch were verified using a different approach in sheet preparations. When imaging the sheet, the depth-of-field of the lens is 100–150 μm. Since the distended rat bladder is 400 to 500 μm thick, signals would come from the underlying smooth muscle and the urothelial-suburothelial layers when the entire preparation was stained and viewed from the mucosal surface. However, by separating the urothelial-suburothelial layers from half of a sheet preparation, we recorded simultaneously signals from *1*) smooth muscle with urothelium-suburothelium, *2*) smooth muscle alone, and *3*) urothelium-suburothelium alone. Stretch-evoked signals were only detected in the urothelial-suburothelial regions of neonatal bladders (n = 4).

DISCUSSION

These experiments have evaluated simultaneous fluorescence transients in the rat bladder using two dyes, rhod 2-AM and di-4-ANNEPS, which measure changes in intracellular Ca^{2+} and membrane potential, respectively. Bladder pressure recordings were similar before and

after staining, demonstrating that there were no adverse effects of the dyes. There was unlikely to be significant cross-talk between the signals because of the sharp attenuation above and below 635 nm, respectively, for the emission spectra of the fluorochromes, so that the final dichroic filter was able to separate the two signals effectively. Moreover, the time courses of the two transients were very different (Fig. 4), showing that separate signals were measured. The signals were unlikely to result from contraction artifacts as similar data were recorded in the presence of 5 mM BDM, an agent that inhibits acto-myosin cross-bridge formation and hence contraction (Fig. 6).

Disparity of Ca^{2+} transient and membrane potential conduction velocities

Ca^{2+} transients and membrane potential changes originated from the same site but propagated at significantly different velocities (neonatal bladder means 3.7 vs. 46.2 mm/s). This implies that Ca^{2+} transients at sites distant from the origin were not merely a consequence of depolarization but that the two signals propagated separately and by different mechanisms. In each case, the signals were nondecremental implying that diffusion alone would not explain their spread. The larger value may be modelled by electrical propagation in a two-dimensional sheet of cells coupled by gap junctions, as was carried out in myocardium (7). Extrapolating this model to the bladder, a propagation velocity of 46 mm/s would be possible through a cellular syncytium if intracellular electrical resistivity was ~1,500–2,000 Ω·cm, a value similar to that measured previously in bladder tissue (26). Propagation of Ca^{2+} waves, after Ca^{2+} release from an initial locus in a discrete population of cells, may be mediated by several mechanisms: for example, by intercellular diffusion of Ca^{2+} to mediate Ca^{2+}-induced Ca^{2+} release (CICR) in neighboring cells; or by physical stretch of adjacent myocytes causing intracellular Ca^{2+} release, due to contraction of a neighbor. Stretch-induced intracellular Ca^{2+} release, sensitive to block by ryanodine, has been demonstrated in isolated detrusor myocytes and multicellular preparations (11) and this coupled to effective CICR in this tissue would provide an effective propagation mechanism. Propagation by intracellular diffusion is a less attractive mechanism, as intracellular diffusion is relatively low at ~20 μm/s (10) and furthermore intercellular propagation of Ca^{2+} waves after stretch was not observed in multicellular detrusor preparations (12). However, the significance of these data is that spontaneous activity of different modalities in the bladder wall spread by a variety of mechanisms and that the magnitude and frequency of such activity will depend on the ability of separate sites to initiate and propagate activity.

Pathological implications of focally initiated large-amplitude spontaneous contractions

In neonatal rats, micturition is mediated by a somato-bladder spinal reflex pathway that is activated by the mother licking their perineum. During development, this primitive reflex is replaced by supraspinal mechanisms which control mature bladder-to-bladder reflexes and voluntary voiding (24,25). This developmental change in the central control of voiding occurs in concert with changes to peripheral neurotransmission and the intrinsic properties of the bladder. In our neonatal bladders, these intrinsic properties included focally initiated activity that began in the dome and spread uniformly throughout the bladder. This resulted in large spontaneous contractions that, in vivo, may enhance afferent firing and promote efferent stimulation and voiding. A previous study measuring spontaneous activity in isolated neonatal bladder strips has suggested that spontaneous activity begins near the outlet (23), because higher frequencies were observed in tissue from that region. The difference between our experiments in whole bladders and those using strips may be related to the fact that isolated strips are prone to damage on removal from the bladder and are subject to varying degrees of resting tension. It is also significant that while organized activity disappears in adult bladders, it reemerges in pathology due to spinal cord transection or bladder outlet obstruction (28), and thus could contribute to urgency, and in a proportion of patients urgency incontinence.

Urothelium as the source and site-of-action of stretch-induced ACh release

The origin of spontaneous signals may be in the smooth muscle or the urothelial-suburothelial layers. Data from transverse sections (Fig. 8) indicated that the latter is an important contributor. We emphasize that voltage and Ca^{2+} signals arising from these different layers could be resolved because we used a magnification where each pixel imaged a 62.5 × 62.5-μm^2 region. As such, the urothelium was imaged by two, the lamina propria by three and the detrusor by nine rows of pixels. We hypothesize that stretch releases ACh from the urothelium, which in turn activates urothelial muscarinic receptors to release ATP and drive spontaneous activity. This agrees with our observations that stretchor carbachol-evoked voltage and Ca^{2+} signals arose in the urothelial-suburothelial layers and then propagated to the detrusor, but only after a delay. Control observations showed that mechanical stretch applied to the detrusor layer elicited no responses and further strengthens the argument that the signals originate in the urothelial-suburothelial layers. Furthermore, while atropine abolished stretch- and carbachol-induced Ca^{2+} transients in the urothelial-suburothelial layers as well as the delayed response in the detrusor, suramin only blocked the detrusor response. The particular cellular arrays wherein such activity is initiated are unclear. However, it may be hypothesized that interstitial cells may have a role, as spontaneous activity is abolished by the *c-kit* tyrosine kinase inhibitor Glivec (15). *C-kit* labeling has been described on interstitial cells (8,19) and further work in this direction should clarify this question.

The resistance of spontaneous activity to TTX block suggests that ACh mediating this response is not released by action potentials in nerve endings. While there could be TTX-resistant ACh release from nerves, a more likely source of ACh would be the urothelium. The high density of urothelial muscarinic receptors, compared with detrusor (6), would support this hypothesis. The data in Fig. 8 further suggest that these receptors are located on the abluminal (basolateral) side of the urothelium. This is quite reasonable since ACh released from the luminal (apical) surface would be rapidly diluted by the large volume of urine. The apical surface of umbrella cells also exhibits high transepithelial resistance and low water and solute permeabilities (13,14), making this surface an unlikely site for transmitter release.

These experiments demonstrated propagating spontaneous waves of intracellular Ca^{2+} and membrane potential generated in the bladder wall that conduct at different velocities and presumably by different mechanisms. Moreover, these waves may be augmented by conditions that are believed to occur during bladder filling, such as bladder wall stretch and release of muscarinic receptor activators. These waves are more coordinated in neonatal compared with adult bladders. The central role of the urothelium and suburothelium in initiating these phenomena suggests that this region of the bladder wall is an important target to control overall bladder activity.

Acknowledgments

This work is funded by National Institutes of Health Grants DK-064280 to A. J. Kanai and DK-054824 to L. A. Birder. C. H. Fry is grateful to the Physiological Society for a traveling grant to Pittsburgh.

REFERENCES

1. Andersson KE. Antimuscarinics for treatment of overactive bladder. Lancet Neurol. 2004; 3:46–53. [PubMed: 14693111]
2. Andersson KE, Chapple C, Wein A. The basis for drug treatment of the overactive bladder. World J Urol. 2001; 19:294–298. [PubMed: 11760776]

3. Andersson KE, Yoshida M. Antimuscarinics and the overactive detrusor-which is the main mechanism of action? Eur Urol. 2003; 43:1–5. [PubMed: 12507537]
4. Brading AF. Spontaneous activity of lower urinary tract smooth muscles: correlation between ion channels and tissue function. J Physiol. 2006; 570:13–22. [PubMed: 16210349]
5. Chapple CR. Muscarinic receptor antagonists in the treatment of overactive bladder. Urology. 2000; 55:33–46. discussion 50. [PubMed: 10767450]
6. Chess-Williams R. Muscarinic receptors of the urinary bladder: detrusor, urothelial and prejunctional. Auton Autacoid Pharmacol. 2002; 22:133–145. [PubMed: 12452898]
7. Cooklin M, Wallis WR, Sheridan DJ, Fry CH. Conduction velocity and gap junction resistance in hypertrophied, hypoxic guinea-pig left ventricular myocardium. Exp Physiol. 1998; 83:763–770. [PubMed: 9782186]
8. Davidson RA, McCloskey KD. Morphology and localization of interstitial cells in the guinea pig bladder: structural relationships with smooth muscle and neurons. J Urol. 2005; 173:1385–1390. [PubMed: 15758810]
9. Hashitani H, Brading AF. Ionic basis for the regulation of spontaneous excitation in detrusor smooth muscle cells of the guinea-pig urinary bladder. Br J Pharmacol. 2003; 140:159–169. [PubMed: 12967945]
10. Jaffe LF. The path of calcium in cytosolic calcium oscillations: a unifying hypothesis. Proc Natl Acad Sci USA. 1991; 88:9883–9887. [PubMed: 1946414]
11. Ji G, Barsotti RJ, Feldman ME, Kotlikoff MI. Stretch-induced calcium release in smooth muscle. J Gen Physiol. 2002; 119:533–544. [PubMed: 12034761]
12. Ji G, Feldman M, Doran R, Zipfel W, Kotlikoff MI. Ca^{2}+-induced Ca^{2}+ release through localized Ca^{2}+ uncaging in smooth muscle. J Gen Physiol. 2006; 127:225–235. [PubMed: 16505145]
13. Kanai A, Epperly M, Pearce L, Birder L, Zeidel M, Meyers S, Greenberger J, de Groat W, Apodaca G, Peterson J. Differing roles of mitochondrial nitric oxide synthase in cardiomyocytes and urothelial cells. Am J Physiol Heart Circ Physiol. 2004; 286:H13–H21. [PubMed: 14684357]
14. Kanai AJ, Zeidel ML, Lavelle JP, Greenberger JS, Birder LA, de Groat WC, Apodaca GL, Meyers SA, Ramage R, Epperly MW. Manganese superoxide dismutase gene therapy protects against irradiation-induced cystitis. Am J Physiol Renal Physiol. 2002; 283:F1304–F1312. [PubMed: 12426235]
15. Kubota Y, Biers SM, Kohri K, Brading AF. Effects of imatinib mesylate (Glivec) as a *c-kit* tyrosine kinase inhibitor in the guinea-pig urinary bladder. Neurourol Urodyn. 2006; 25:205–210. [PubMed: 16425211]
16. Kumar V, Templeman L, Chapple CR, Chess-Williams R. Recent developments in the management of detrusor overactivity. Curr Opin Urol. 2003; 13:285–291. [PubMed: 12811292]
17. Maggi CA, Santicioli P, Meli A. Postnatal development of myogenic contractile activity and excitatory innervation of rat urinary bladder. Am J Physiol Regul Integr Comp Physiol. 1984; 247:R972–R978.
18. Maggi CA, Santicioli P, Meli A. The effect of urethane on spontaneous and stimulated contractions of isolated rabbit urinary bladder. Arch Int Pharmacodyn Ther. 1984; 271:293–302. [PubMed: 6508436]
19. McCloskey KD, Gurney AM. Kit positive cells in the guinea pig bladder. J Urol. 2002; 168:832–836. [PubMed: 12131376]
20. Nijman RJ. Role of antimuscarinics in the treatment of nonneurogenic daytime urinary incontinence in children. Urology. 2004; 63:45–50. [PubMed: 15013652]
21. Osterman A, Arner A, Malmqvist U. Effects of 2,3-butanedione monoxime on activation of contraction and crossbridge kinetics in intact and chemically skinned smooth muscle fibres from guinea pig *taenia coli*. J Muscle Res Cell Motil. 1993; 14:186–194. [PubMed: 8315022]
22. Rovner ES, Wein AJ. Once-daily, extended-release formulations of antimuscarinic agents in the treatment of overactive bladder: a review. Eur Urol. 2002; 41:6–14. [PubMed: 11999467]
23. Sugaya K, de Groat WC. Influence of temperature on activity of the isolated whole bladder preparation of neonatal and adult rats. Am J Physiol Regul Integr Comp Physiol. 2000; 278:R238–R246. [PubMed: 10644645]

24. Sugaya K, de Groat WC. Inhibitory control of the urinary bladder in the neonatal rat in vitro spinal cord-bladder preparation. Brain Res Dev Brain Res. 2002; 138:87–95.
25. Sugaya K, De Groat WC. Micturition reflexes in the in vitro neonatal rat brain stem-spinal cord-bladder preparation. Am J Physiol Regul Integr Comp Physiol. 1994; 266:R658–R667.
26. Sui GP, Coppen SR, Dupont E, Rothery S, Gillespie J, Newgreen D, Severs NJ, Fry CH. Impedance measurements and connexin expression in human detrusor muscle from stable and unstable bladders. BJU Int. 2003; 92:297–305. [PubMed: 12887488]
27. Szell EA, Somogyi GT, de Groat WC, Szigeti GP. Developmental changes in spontaneous smooth muscle activity in the neonatal rat urinary bladder. Am J Physiol Regul Integr Comp Physiol. 2003; 285:R809–R816. [PubMed: 12750150]
28. Szigeti GP, Somogyi GT, Csernoch L, Szell EA. Age dependence of the spontaneous activity of the rat urinary bladder. J Muscle Res Cell Motil. 2005; 26:23–29. [PubMed: 16025204]
29. Yono M, Yoshida M, Takahashi W, Inadome A, Ueda S. Comparison of the effects of novel antimuscarinic drugs on human detrusor smooth muscle. BJU Int. 2000; 86:719–725. [PubMed: 11069384]
30. Yoshida M, Inadome A, Maeda Y, Satoji Y, Masunaga K, Sugiyama Y, Murakami S. Nonneuronal cholinergic system in human bladder urothelium. Urology. 2006; 67:425–430. [PubMed: 16461116]
31. Yossepowitch O, Gillon G, Baniel J, Engelstein D, Livne PM. The effect of cholinergic enhancement during filling cystometry: can edrophonium chloride be used as a provocative test for overactive bladder? J Urol. 2001; 165:1441–1445. [PubMed: 11342893]

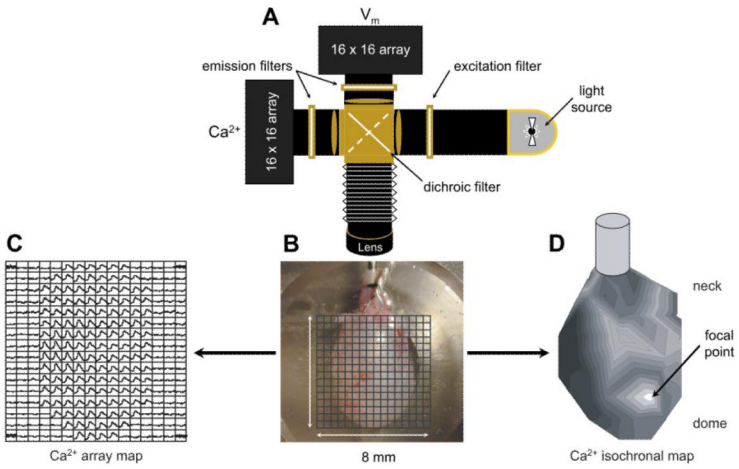

Fig. 1.

Optical system to record intracellular Ca^{2+} and membrane potential signals from bladder preparations. *A*: optical system showing the arrangement of the light source, filters, and photodiode arrays. *B*: neonatal bladder observed in situ with a 16 × 16 array grid superimposed to show the individual photodiode recording fields. *C*: Ca^{2+} signals recorded from the photodiode array, the observed transient signals correspond to the field occupied by the bladder surface in *B*. The recording duration was 60 s. *D*: isochronal map derived from the data in *C*. The initiation site was identified as the individual signal in *C* with the earliest Ca^{2+} transient ("focal point" in *D*). The neck-to-dome axis is shown from *top* to *bottom*. Isochrones represent successive conduction delays of 44 ms (*D*).

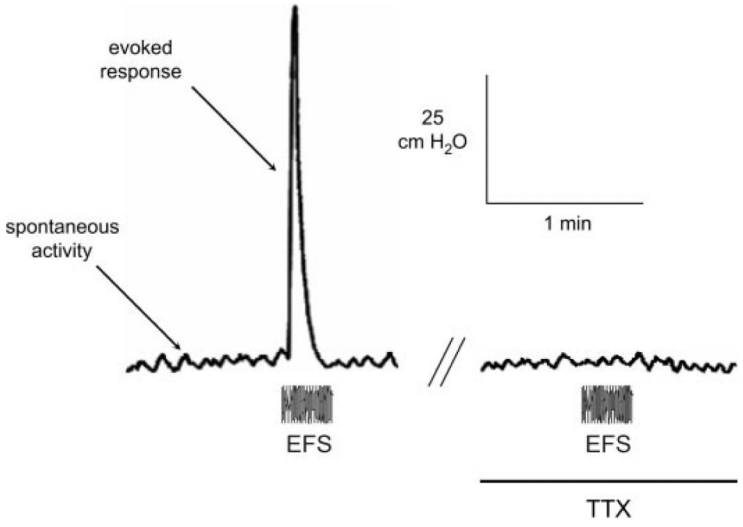

Fig. 2.

Intravesical pressure transients recorded from a whole adult bladder before and after addition of 2 μM tetrodotoxin (TTX). The period of electrical stimulation (EFS; 20-s trains, 50 Hz, 0.25 ms, 140-V pulses) is shown.

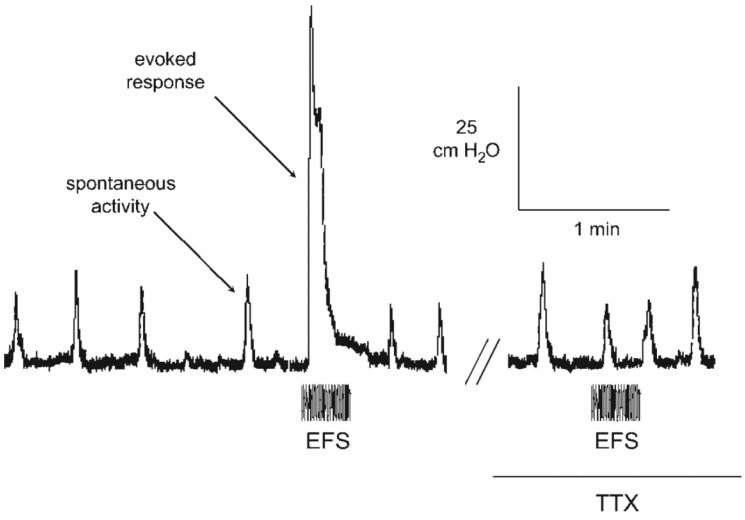

Fig. 3.

Intravesical pressure transients recorded from a neonatal bladder before and after addition of 2 μM TTX. The layout and period of electrical stimulation are similar to that of Fig. 2.

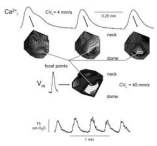

Fig. 4.

Ca^{2+} and membrane potential transients in the neonatal rat bladder. *Top* traces: successive Ca^{2+} transients above the corresponding isochronal maps. *Middle* trace: membrane potential transient and the associated isochronal map corresponding to *middle* Ca^{2+} transient above. *Bottom* traces: spontaneous intravesical pressure changes, with the *middle* 3 corresponding to the Ca^{2+} and the *middle* one corresponding to the membrane potential transients shown above. Isochrones represent successive conductions delays of 44 ms for the Ca^{2+} array and 4 ms for the membrane potential array.

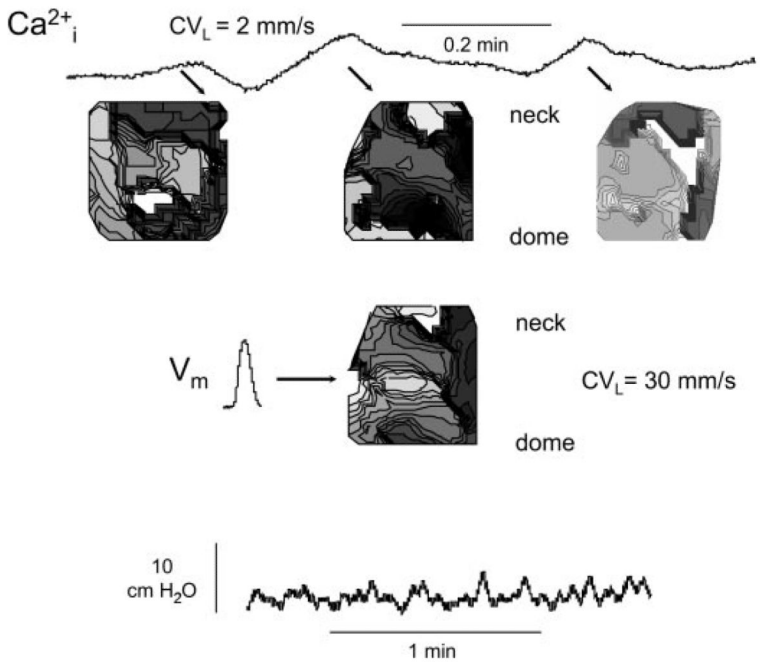

Fig. 5.

Ca^{2+} and membrane potential transients in the adult rat bladder. The layout is similar to that of Fig. 4. Isochrones represent successive conductions delays of 89 ms for the Ca^{2+} array and 6 ms for the membrane potential array.

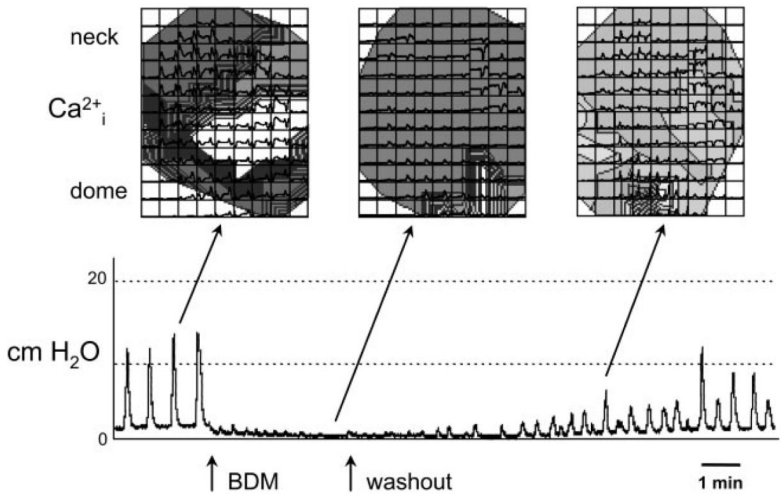

Fig. 6.

Ca^{2+} maps in the presence of 2,3-butanedione monoxamine (BDM). *Bottom*: effect of 5 mM BDM on the pressure recording from an intact neonatal rat bladder. *Top*: spontaneous Ca^{2+} trace data superimposed over isochronal maps generated from these intracellular Ca^{2+} transients. While BDM abolished smooth muscle contractile activity, and therefore bladder pressure generation, spontaneous Ca^{2+} transients persisted.

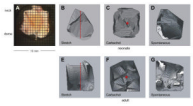

Fig. 7.

Ca^{2+} maps in sheets of bladder from neonatal (*A–D*) and adult (*E–G*) rats. *A*: bladder sheet from a neonatal rat with the mucosal face uppermost and a superimposed photodiode array grid. The positions of the dome and neck of the bladder are shown. *B* and *E*: isochronal Ca^{2+} maps after stretch (0.8 mm or 10%) in the neck-dome axis, indicated by the double headed arrows. *C* and *F*: isochronal Ca^{2+} maps after the topical application of carbachol (50 nM), indicated by *. *D* and *G*: spontaneous isochronal Ca^{2+} maps. Isochrones represent successive conduction delays of 44 ms (*B–D*) and 89 ms (*E–G*).

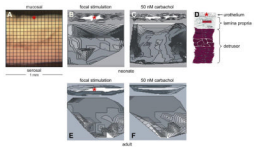

Fig. 8.

Ca^{2+} maps in bladder transverse sections from neonatal (*A–C*) and adult (*E–F*) rats. *A*: transverse section of a neonatal rat bladder, the mucosal and serosal surfaces are shown. *B* and *E*: isochronal Ca^{2+} maps after point mechanical stimulation at the sites marked by *. *C* and *F*: isochronal Ca^{2+} maps after topical application of carbachol (50 nM). *D*: diagram of the bladder wall on the same transverse scale as in *A–C* and *E–F*. Isochrones represent successive conduction delays of 7 ms (*B–C*) and 15 ms (*E–F*).